ARKIV FÖR FYSIK Band 19 nr 3

Communicated 12 October by B. Edlén and T. Gustafson

A three crystal pair spectrometer

By L. Ask, B. Erlandsson, B. Persson and K. Valli

With 11 figures in the text

ABSTRACT

The construction of a scintillation pair spectrometer of high efficiency and good energy resolution is described. Its response function for energies below 18 MeV is obtained and the variation of this response, due to different collimations of incident radiation and the use of central crystals of different lengths, is studied.

Introduction

The principle of the three crystal pair spectrometer was pointed out by Hofstadter and McIntyre, and Johansson [1, 2]. Its most important properties, compared with the usual scintillation spectrometer, e.g. its better resolution and simpler response function, are clearly demonstrated in Fig. 5. The first instrument of this kind was constructed by Johansson [2, 3], followed by several others [4–12]. In these instruments one was restricted to the use of small to moderately sized crystals, and as a consequence, their efficiency was low, and they were suited to the study of high intensity radiation only. For use in connection with weaker radiation, spectrometers with larger side crystals (3 inches in diameter) have been used [13–15].

In the following we describe the construction of a three crystal pair spectrometer of high efficiency using side crystals each with a diameter of 5 inches. Its response to different γ-lines in the energy range 2.6 to 17.6 MeV is investigated. The influence of different collimations is studied, as well as the effect of different sizes of the central crystal on the spectrometer's performance.

Apparatus

Schematic diagrams of the apparatus are shown in Figs. 1 and 2. The radiation under investigation must pass through a lead collimator before reaching the central detector (D1). Different collimators were used. When there was a rather large distance between the source and the central crystal, we used collimators of 175 mm length, one with a cylindrical hole (C1) whose diameter was 18 mm, and another (C2) with a conical hole, the diameters at the ends of which were 18 and 10 mm. When the distance was shorter, a double conical collimator (C3) was used. Its dimensions are given in Fig. 1. As central detector we used a crystal, 1.5 inches in diameter and 3 inches long, coupled to a photomultiplier (DuMont 6292).

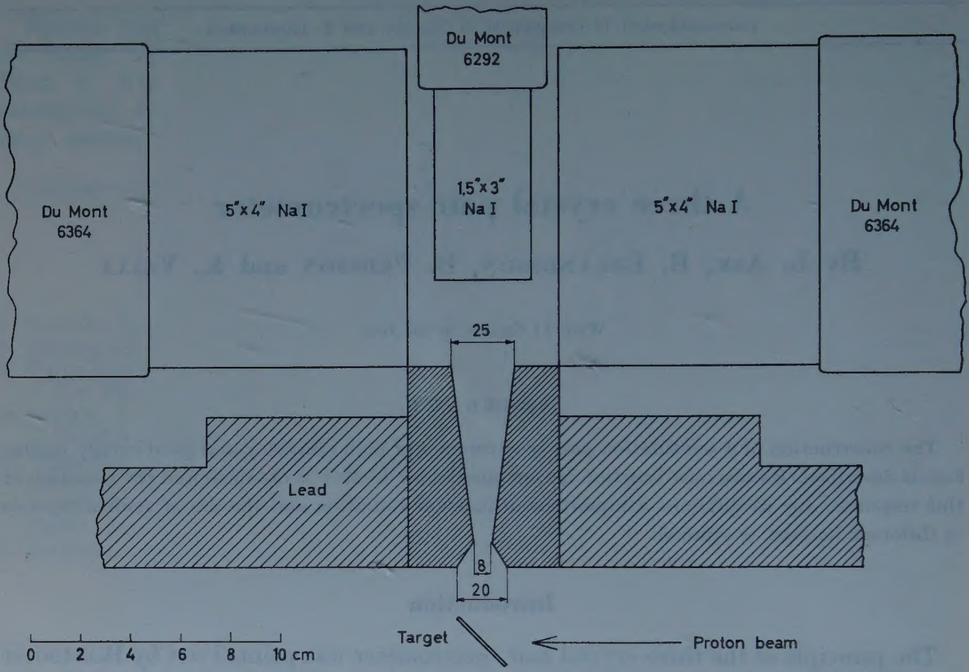

Fig. 1. Schematic diagram of experimental arrangements with the double conical collimator (C3).

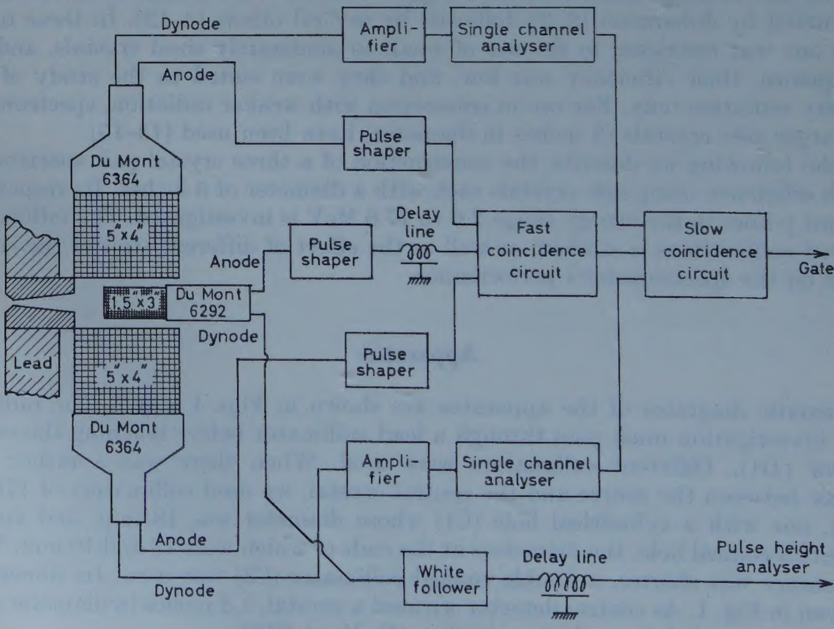

Fig. 2. Block diagram of the electronics.

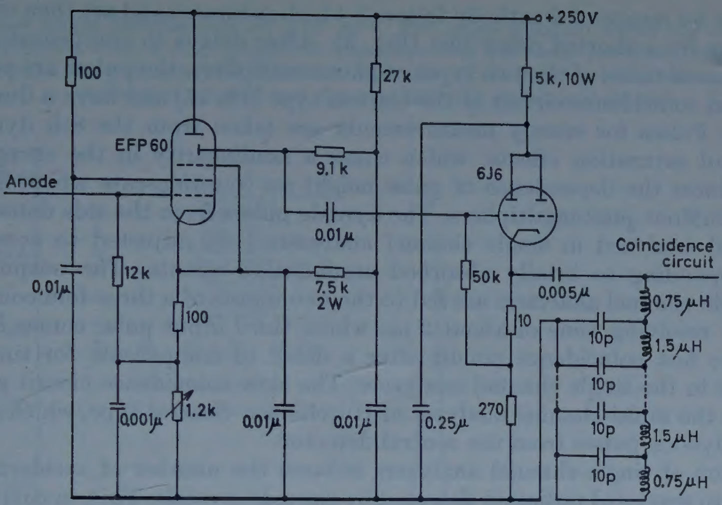

Fig. 3. Pulse-shaping circuit. It produces a narrow pulse, corresponding to the start of light emission in the crystal. The negative pulse from the photomultiplier anode is amplified without inversion in the secondary emission tube EFP60. It then drives the cathode follower (6J6) to cut-off. The result is a fast-rising, amplitude standardized output pulse, which is reflected in the shorted delay line, giving a standardized short (~50 ns) output pulse.

The dimensions of the collimators and of the central crystal were chosen so as to get a reasonably large irradiated volume of the central crystal. This volume must be so located that its distance to the cylindrical surface of the crystal is long enough to prevent most of the electrons and positrons from pair events from escaping out of the crystal. At the same time the absorption of annihilation quanta within the central crystal must be small. These factors affect the energy resolution as well as the efficiency of the instrument and as the conditions are contradictory, there is an optimum choice. The diameters of the two long collimators were estimated to give the best energy resolution. With the short collimator better efficiency is obtained by a sacrifice of resolution. The unusual length of the central crystal, compared with those for ordinary scintillation spectrometric use, is explained by our effort to minimize the escape of electrons and positrons, as well as the bremsstrahlung quanta they produce, through the crystal's back surface. In some experiments for comparison a crystal, 1.75 inches in diameter and 1 inch long, served in the central detector.

The central crystal is surrounded by two side detectors (D2 and D3) with crystals, 5 inches in diameter and 4 inches long, coupled to DuMont 6364 photomultipliers. The large diameters of these crystals make a high detection probability of annihilation quanta possible and consequently give a good efficiency for the instrument as a whole. All crystals used are thallium-activated sodium iodide crystals supplied and mounted by Harshaw.

The purpose of the electronic equipment is to produce an opening pulse to the gate of the multi-channel analyzer only for those pulses in the central detector which correspond to pair production. It is essentially a fast–slow coincidence arrangement. The pulses for the fast three-fold coincidence circuit are taken from the anodes of the photomultipliers and are amplified in secondary emission tubes. They are standardized in height by means of a cathode follower which saturates and are then clipped in the usual way by a shorted delay line (Fig. 3). After delays to compensate for differences in transit times of the two types of photomultipliers, the pulses are presented to a three-fold coincidence circuit of the Garwin type [16, 17] and have a duration of about 50 ns. Pulses for energy measurements are taken from the 8th dynodes in order to avoid saturation effects, which cause a nonlinearity in the energy scale. This also reduces the dependence of pulse height on counting rate which is known to occur in DuMont photomultipliers. The dynode pulses from the side detectors are amplified and analyzed in single channel analyzers [18], adjusted to accept only pulses corresponding to totally absorbed annihilation quanta. The output pulses from the single-channel analyzers are fed to the two inputs of a three-fold coincidence circuit, with resolving time of about 2 μs, whose third input pulse comes from the output of the fast coincidence circuit after a delay to compensate for time spent by the pulses in the single channel analyzers. The slow coincidence circuit gives the gate pulse to the multi-channel analyzer of Hutchinson–Scarrot type, which analyzes the delayed dynode pulses from the central detector.

The addition of single channel analyzers reduces the number of accidental coincidences due to scattered radiation detected by the side crystals. This, in combination with the short resolving time used, made it possible to neglect the accidental coincidences in investigations made so far.

Performance

The performance of the spectrometer at different energies was investigated and as radiation sources we used RdTh and the reactions $F^{19}(p, \alpha\gamma)O^{16}$, $B^{11}(p, \gamma)C^{12}$, and $Li^7(p, \gamma)Be^8$ [19]. The protons were accelerated in a van de Graaff generator and the γ-radiation at an angle of 90° to the proton beam was used.

RdTh. This source gives 2.62 MeV γ-radiation in addition to radiation of lower energies to which the spectrometer does not respond.

$F^{19}(p, \alpha\gamma)O^{16}$. A thick target of calcium fluoride was used. The proton energy was kept at 400 keV to give γ-radiation of almost pure 6.14 MeV from the resonance at 340 keV proton energy.

$B^{11}(p, \gamma)C^{12}$. This reaction gives 4.43, 11.7, and 16.1 MeV γ-radiation and was used to obtain the response function for both 4.43 and 11.7 MeV γ-radiation. A deposit of boron on a copper plate was used as target. During the 4.43 MeV runs the proton energy was maintained at 800 keV and during the 11.7 MeV runs at 550 keV.

$Li^7(p, \gamma)Be^8$. A thick target of metallic lithium was used. The proton energy was at 700 keV, which yields γ-radiation of energies 14.8 and 17.6 MeV from the resonance at 441 keV proton energy.

2.62 MeV. The general appearance of the pulse height distribution is shown in Fig. 4, were the geometric arrangement is also indicated, the long cylindrical collimator (Cl) being used. With this collimator the distance between the source and the central crystal was varied and the effect is shown down to the left in this figure, where the tails of the distributions are drawn to an expanded scale. The ordinate gives the height in per cent of the top value. The relative appearance of the peaks for different distances is shown down to the right with the peaks normalized to the same height. The widths of the peaks are tabulated in Table 1. By width we mean, here and in the following, the width of the distribution at half its maximum value. The

Fig. 4. Pulse height distributions for 2.62 MeV. The upper diagram shows the complete pulse height distribution when a long cylindrical collimator (C1) was used. The lower diagrams show in expanded scales the peaks, to the right, and the tails, to the left, for different combinations of collimator, crystal and distance between source and crystal.

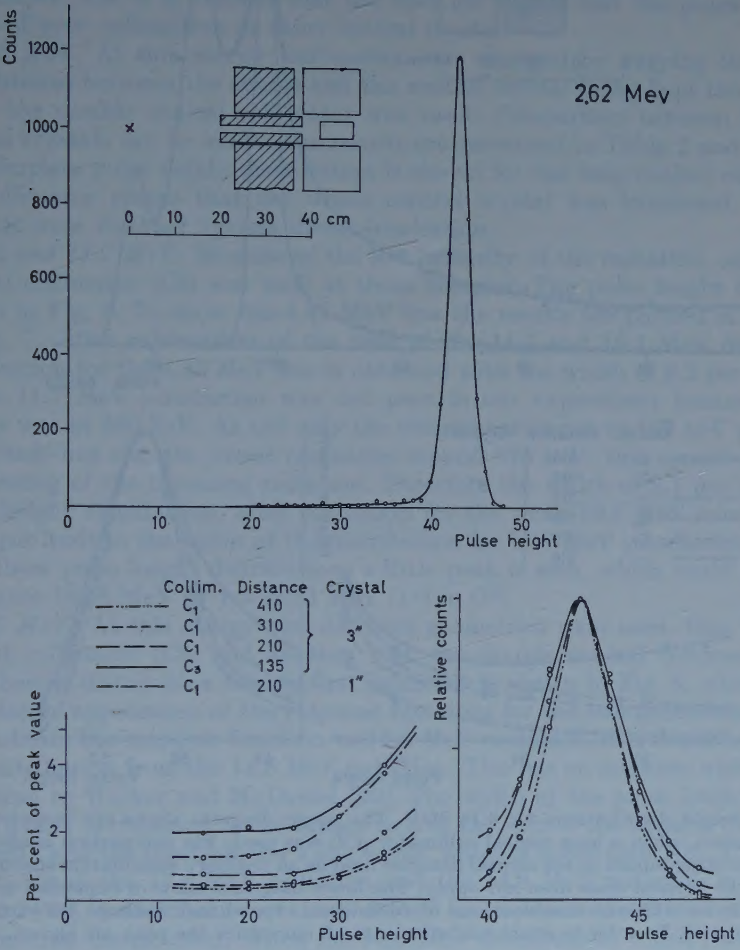

Table 1. The relative widths $\Delta E/(E\gamma - 1.02)$ and $\Delta E/E\gamma$ at $E\gamma = 2.62$ MeV.

Crystal	1″	3″			
Collimator	C_1	C_1			C_3
Distance, mm	210	210	310	410	135
$\Delta E/(E\gamma - 1.02)$, % $\Delta E/E\gamma$, %	8.0 5.0	6.6 4.1	6.3 3.9	5.8 3.6	8.0 5.0

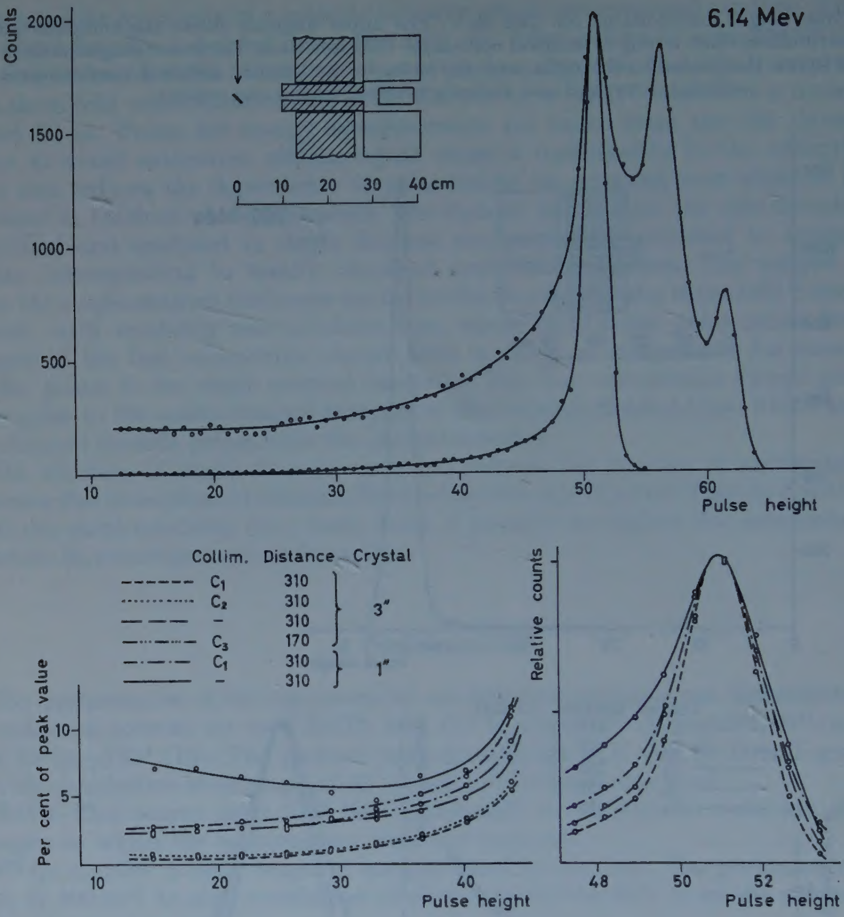

Fig. 5. Pulse height distributions for 6.14 MeV. The upper diagram shows the complete pulse height distribution, when a long conical collimator (C2) was used. For comparison is also shown the pulse height distribution in the central detector used as an ordinary scintillation spectrometer. In that case, the vertical scale does not apply. The lower diagrams show in expanded scales the peaks and tails for different combinations of collimator, crystal and distance between source and crystal. In order to avoid confusion, not all curves for the peak are shown.

Table 2. The relative widths $\Delta E/(E\gamma - 1.02)$ and $\Delta E/E\gamma$ at $E\gamma = 6.14$ MeV.

Crystal	1″		3″			
Distance, mm	310		310			170
Collimator	–	C_1	–	C_1	C_2	C_3
$\Delta E/(E\gamma-1.02)$, %	7.5	5.7	5.0	4.4	4.2	5.2
$\Delta E/E\gamma$, %	6.3	4.8	4.2	3.7	3.5	4.3

influence of the size of the central crystal is seen by comparison with the curve for the run where a 1 inch crystal was used in connection with the same collimator and the shortest distance. There is also a curve for a quite different geometry, the double conical collimator (C3) and a short distance. These curves have all the same general appearance, but it is evident that the tails get higher and the peaks broader as a result of poor collimation or short central crystal.

6.14 MeV. At this energy, collimation was changed by varying the collimators, the distance between the source and the central crystal being kept the same, except when the double conical collimator was used. Comparison between 1 and 3 inch central crystals can be made. The results are presented in Table 2 and Fig. 5, where the complete pulse height distribution is shown for the long conical collimator (C2). No collimator means that the whole central crystal was irradiated, but the side crystals were shielded against direct irradiation.

4.43 and 11.7 MeV. Because of the low intensity of the radiation, only the double conical collimator (C3) was used at these energies. The pulse height distribution is shown in Fig. 6. To show the 4.43 MeV line the results are plotted in another scale in Fig. 7. After subtraction of the tails of the 11.7 and 16.1 MeV distributions, a distribution for the 4.43 MeV line is obtained with the width of 6.2 per cent.

The 11.7 MeV γ-radiation was not pure in our experiment because the proton energy was at 550 keV. As not only the desired resonance at 163 keV proton energy is excited, but also the broad resonance around 675 keV, this contributes to give a broadening of the incoming radiation. Therefore the width of 8.7 per cent from the pulse height distribution, after correction for the weak 16.1 MeV component, gives an upper limit to the width of the distribution for 11.7 MeV γ-radiation.

In these pulse height distributions a little peak is seen, which could be due to the transition 16.58 MeV $(2^-) \rightarrow 12.73$ MeV (1^+) in C^{12}.

17.6 MeV. At this energy two different geometries were used. One with the long conical collimator (C2) and another with the double conical collimator (C3). The pulse height distribution for the first geometry is shown in Fig. 8, which also shows the relative appearance of the response functions for the two geometries.

To obtain the response function to 17.6 MeV radiation, it is necessary to subtract the contribution from the 14.8 MeV radiation. This has an intrinsic width of 2.1 MeV according to Walker and McDaniel [20]. The width of the pulse height distribution for 14.8 MeV is obtained as the square root of the sum of the squares of this intrinsic line width and the spectrometer's line width, which is taken from Fig. 9. The intensity ratio between the 17.6 MeV radiation and the 14.8 MeV radiation is known to be 1.7 ± 0.2 [21]. A distribution of the 17.6 MeV line is assumed and subtracted from the experimental distribution. When the 14.8 MeV distribution, which results after correction for the spectrometer's efficiency, has the area and the width satisfying the conditions mentioned above, the assumed 17.6 MeV distribution is considered to be the right. In this way, the width obtained with our good collimator (C2) is 13 % and with the poor 21 %. The tail of the distribution is essentially higher for poor collimation than for good.

The variation of the relative width is presented in Fig. 9. The figure shows both the variation of $\Delta E/E\gamma$ and of $\Delta E/(E\gamma - 1.02)$ with $E\gamma$ in order to avoid confusion. Both these quantities are used in the literature to define resolution. ΔE is the width in MeV of the response function at half maximum height and $E\gamma$ is the energy in MeV of the incident radiation. It is seen that below about 6 MeV $\Delta E/(E\gamma - 1.02)$ decreases with increasing $E\gamma$, consistent with its $1/\sqrt{E\gamma}$ dependence at low energies.

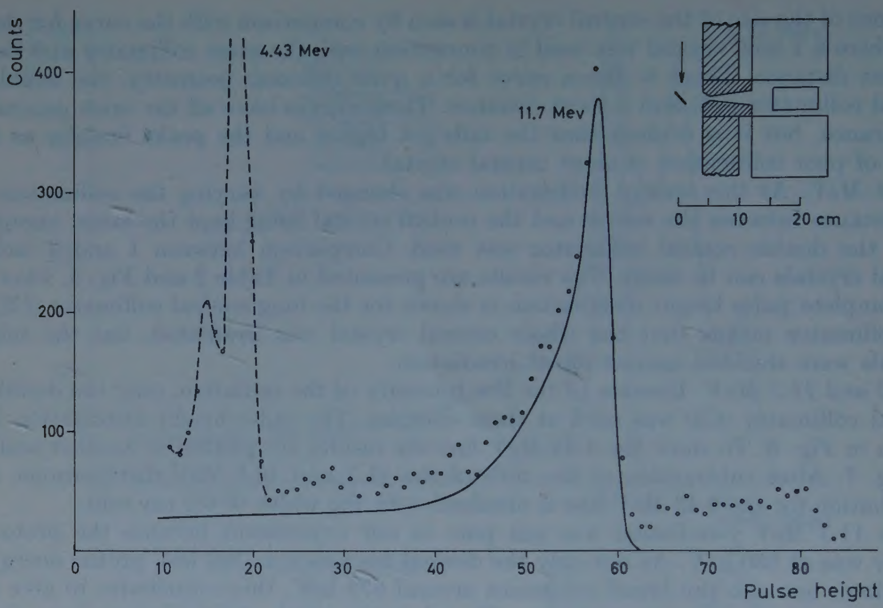

Fig. 6. Pulse height distribution from the reaction $B^{11}(p,\gamma)C^{12}$ and the response function for 11.7 MeV (solid curve).

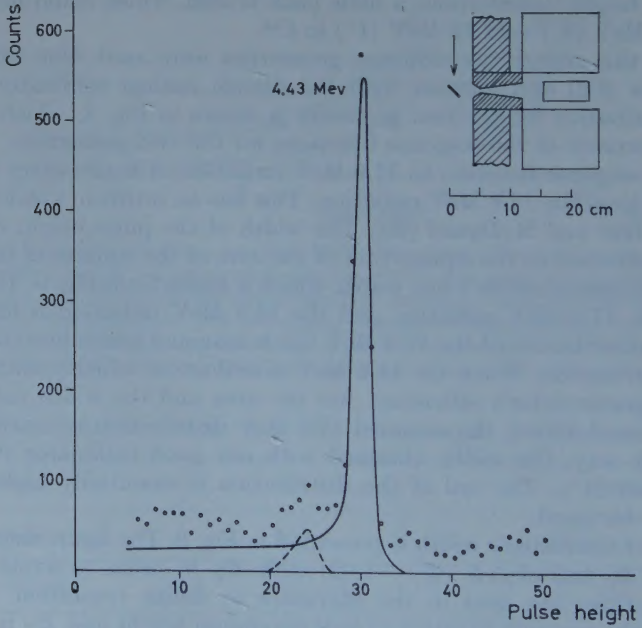

Fig. 7. Part of the pulse height distribution from the reaction $B^{11}(p,\gamma)C^{12}$ and the response function for 4.43 MeV (solid curve). A peak is also shown (dashed curve), which is probably due to the transition 16.58 MeV $(2^-)\rightarrow 12.73$ MeV (1^+) in C^{12}.

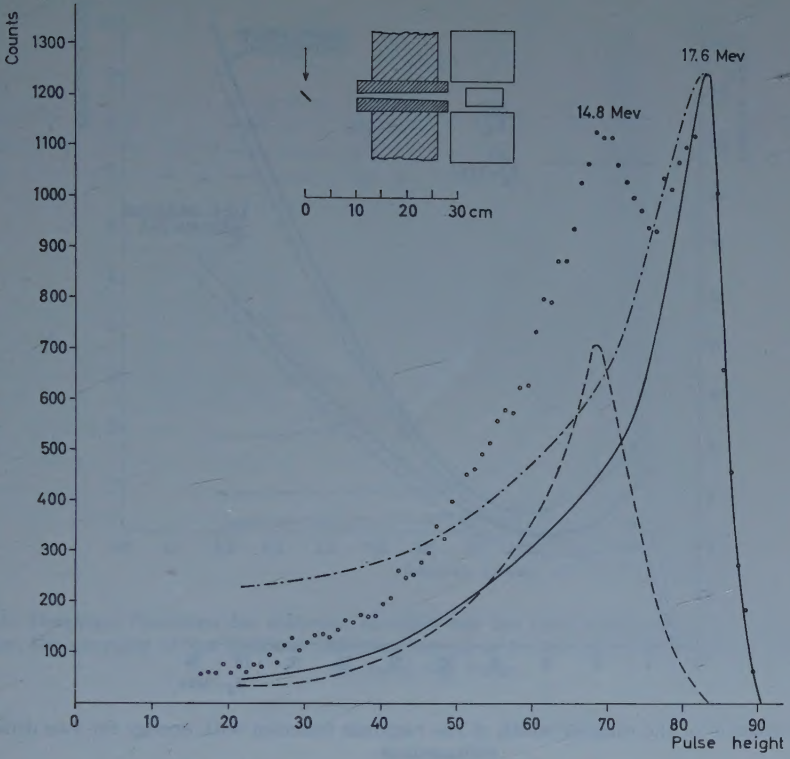

Fig. 8. Pulse height distribution from the reaction $Li^7(p, \gamma)Be^8$ with the long conical collimator (C2) and the response function for 17.6 MeV (solid curve). The dashed curve is the response function for 14.8 MeV. The dot-and-dash curve is the response function for 17.6 MeV obtained with the double conical collimator (C3). Corresponding pulse height distribution is not shown.

Above this energy the escape of bremsstrahlung and particles becomes more and more important, strongly broadening the peak at higher energies. At the same time the tails are raised. This is clearly seen in Fig. 10, where the response functions for various energies and the double conical collimator are shown. With regard to the part of the response functions which corresponds to pulse heights larger than the peak value, the following trend is seen. As the energy rises from 2.62 MeV to 6.14 MeV, the high energy side of the peak goes steeper to zero, as would be expected from the increase, with increasing energy, of the number of photoelectrons ejected from the photocathode. But at further increase of energy, the slope of the high energy side gets smaller. This is evidently due to the escape of bremsstrahlung, which reduces the most probable energy collected by the central crystal. A consequence of this is that the relation between the energy of the incoming radiation and the pulse height for the peak is not quite linear at high energies. Of the collimations used, the deviation from linearity is the largest for the response functions in Fig. 10. In that case it is estimated that the pulse height for the peak at 17.6 MeV would have a value, which differs not more than about 7 % from that expected from the extrapolation of the linear relation at lower energies.

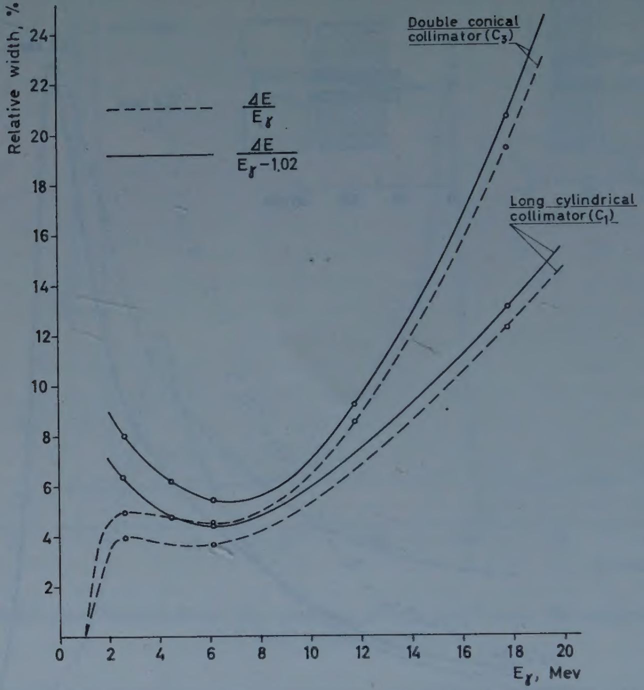

Fig. 9. The variation of the relative width of the response function with energy for two different collimations.

In order to get an estimate of the spectrometer's efficiency a collimated beam with N_0 quanta incident upon the cental crystal is considered. In an element of length dx located at a distance x behind the front surface of the crystal are produced dN electron–positron pairs:

$$d\,N = N_0\,\mathrm{e}^{-\mu_T x}\,\mu_P\,d\,x,$$

where μ_T is the total attenuation coefficient and μ_P is the absorption coefficient for pair production. The number of pair events, dN_P, which is detected is given by

$$d\,N_P = f\,(x)\,N_0\,\mathrm{e}^{-\mu_T x}\,\mu_P\,d\,x.$$

$f(x)$ depends on the position within the central crystal where the pair is created and contains: (1) the probability that the positron is annihilated within the central crystal, (2) the probability that annihilation quanta are not absorbed in the central crystal, and (3) the probability of total absorption of annihilation quanta in the side crystals. Essentially (1) is dependent on the energy of the incident γ-radiation. $f(x)$ is assumed to be constant, however ($f(x) = \bar{f}$) and after integration we obtain

$$N_P = N_0\,\bar{f}\,(1 - \mathrm{e}^{-\mu_T L})\,\mu_P/\mu_T,$$

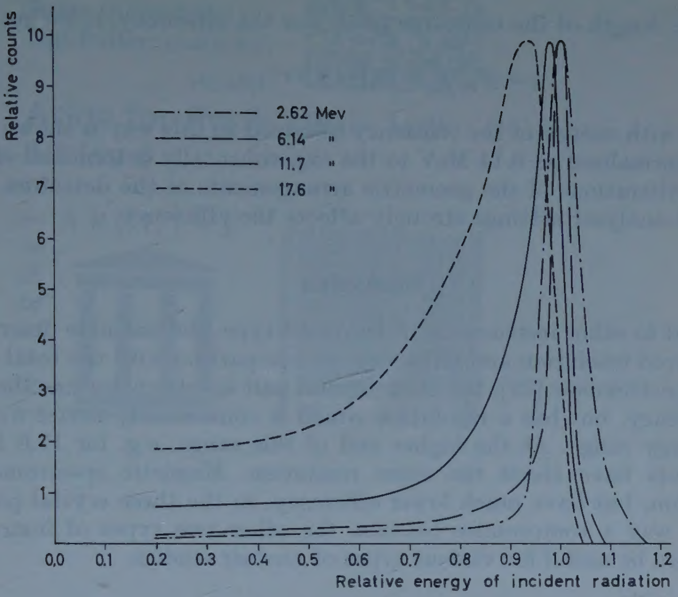

Fig. 10. Response functions for different energies but the same collimation. The energy scale is relative, the energies of the incident radiation are equal to one, and the peaks are normalized to the same top value.

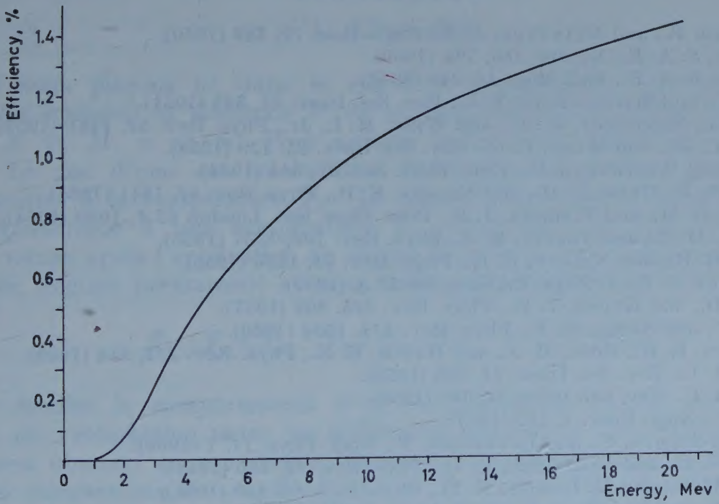

Fig. 11. Efficiency as function of energy. The curve is calculated but is normalized to the experimentally determined efficiency of 0.7 % at 6.14 MeV.

where L is the length of the central crystal. For the efficiency, ε, we get the following relation

$$\varepsilon = N_P/N_0 = f\,(1 - e^{-\mu_T L})\,\mu_P/\mu_T.$$

The variation with energy of the efficiency obtained in this way is shown in Fig. 11. The curve is normalized at 6.14 MeV to the experimentally determined efficiency of 0.7 per cent. Alterations of the geometric arrangements of the detectors and of the single channel analyzer settings strongly affects the efficiency.

Discussion

As compared to other instruments of the same type, the one here described seems to have improved resolution and efficiency. In comparison with the total absorption scintillation spectrometer [22], the three crystal pair spectrometer has the drawback of lower efficiency, but has a resolution which is considerably better over most of its usable energy range. At the higher end of this range, e.g. for 17.6 MeV, these two instruments have about the same resolution. Magnetic spectrometers show better resolution, but have much lower efficiency, so the three crystal pair spectrometer is in a way a compromise between the other two types of instruments. It should therefore be useful for various types of nuclear studies.

ACKNOWLEDGEMENTS

The authors are greatly indebted to Dr. S. A. E. Johansson for his proposal of this work and for valuable discussions. The authors also wish to thank Professor S. von Friesen for his kind interest in the work and for the experimental facilities he has made available.

Department of Physics, University of Lund

REFERENCES

1. Hofstadter, R., and McIntyre, J. A., Phys. Rev. *79*, 389 (1950).
2. Johansson, S. A. E., Nature, *166*, 794 (1950).
3. Johansson, S. A. E., Phil. Mag; *43*, 249 (1952).
4. Bair, J. K., and Maienschein, F. C., Rev. Sci. Instr. *22*, 343 (1951).
5. Mann, L. G., Meyerhof, W. E., and West, H. I., Jr., Phys. Rev. *92*, 1481 (1953).
6. West, H. I., Jr., and Mann, L. G., Rev. Sci. Instr. *25*, 129 (1954).
7. Hird, B., and Whitehead, C., Proc. Phys. Soc. *67*, 644 (1954).
8. Carlson, R. R., Geer, E. H., and Nelson, E. B., Phys. Rev. *94*, 1311 (1954).
9. Griffiths, G. M., and Warren, J. B., Proc. Phys. Soc. London *65 A*, 1050 (1954).
10. Alburger, D. E., and Toppel, B. J., Phys. Rev. *100*, 1357 (1955).
11. Carlson, R. R., and Nelson, E. B., Phys. Rev. *98*, 1310 (1955).
12. Longequeue, J. P., J. Phys. Radium, *20*, 37 A (1959).
13. Bent, R. D., and Kruse, T. H., Phys. Rev. *108*, 802 (1957).
14. Kienle, P., and Segel, R. E., Phys. Rev. *114*, 1554 (1959).
15. Warburton, E. K., Rose, H. J., and Hatch, E. N., Phys. Rev. *114*, 214 (1959).
16. Garwin, R. L., Rev. Sci. Instr. *21*, 569 (1959).
17. Garwin, R. L., Rev. Sci. Instr. *24*, 618 (1953).
18. Åström, B., Nucl. Instr. *1*, 143 (1957).
19. Ajzenberg-Selove, F., and Lauritsen, T., Nucl. Phys. *11*, 1 (1959).
20. Walker, R. L., and McDaniel, B. D., Phys. Rev. *74*, 315 (1948).
21. Stearns, M. B., and McDaniel, B. D., Phys. Rev. *82*, 450 (1951).
22. Kockum, J., and Starfelt, N., Nucl. Instr. *4*, 171 (1959).

Tryckt den 27 januari 1961

Uppsala 1961. Almqvist & Wiksells Boktryckeri AB